Separation of the charge transfers and solid electrolyte interphase contributions to a battery voltage by modeling their non-linearities regarding current and temperature

Nicolas Damay, Karrick Mergo Mbeya, Guy Friedrich, Christophe Forgez

Graphical Abstract

Separation of the charge transfers and solid electrolyte interphase contributions to a battery voltage by modeling their non-linearities regarding current and temperature

Nicolas Damay, Karrick Mergo Mbeya, Guy Friedrich, Christophe Forgez

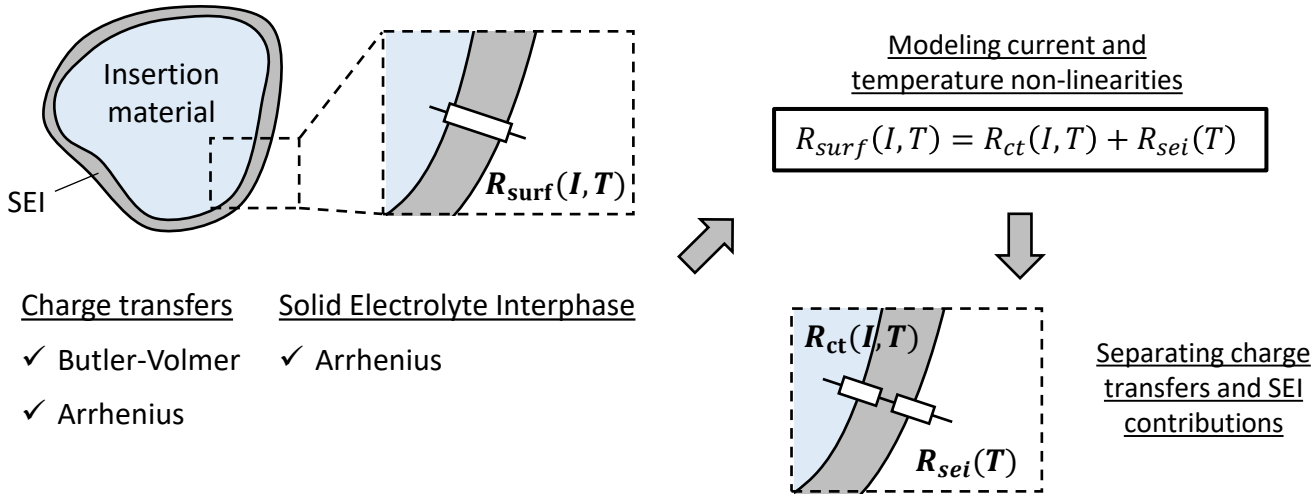

Separation of the charge transfers and solid electrolyte interphase contributions to a battery voltage by modeling their non-linearities regarding current and temperature

Nicolas Damay[a,*], Karrick Mergo Mbeya[a], Guy Friedrich[a], Christophe Forgez[a]

[a] *Université de Technologie de Compiègne, Roberval (Mechanics, energy and electricity) Centre de recherche Royallieu, CS 60319, 60203 Compiègne Cedex, France*

Abstract

One major aging phenomenon during the normal operation of a Li-ion battery is the thickening of its anode solid electrolyte interphase (SEI), which affects the battery state of health. However, the diagnosis of this SEI is difficult because its contribution to the battery voltage is mixed with those of other phenomena. In this article, a method is proposed to separate the contributions of charge transfers and anode SEI. It is based on EIS and GITT measurements and on a model of the charge transfers and SEI non-linearities regarding current and temperature, inspired by Butler-Volmer and Arrhenius equations. The proposed method is applied to a commercial $LiFePO_4$/graphite cell. The activation energies of its SEI and charge transfers resistances are respectively 0.59 eV and 0.81 eV, which is in accordance with literature data. By construction, the method should be applicable to other battery chemistries, unless their cathode SEI has a significant resistive contribution. After an initial calibration, the proposed model can be embedded in a BMS. The latter may then be able to recalibrate the model online thanks to currents pulses at low temperatures and thus track the SEI growth of a battery during its entire operating life.

Keywords: Battery ; modeling ; electrical circuit model ; charge transfer ; SEI ; non-linearities

1. Introduction

Lithium-ion batteries (LIB) aging is a major concern because it impacts their lifetime and performance and one major aging phenomenon during normal operation is the thickening of the anode solid electrolyte interphase (SEI). The SEI is a passivation layer on the anode surface that is created at the end of a battery production and it is mandatory for the battery to work properly. However, this SEI grows endlessly during the battery life, because of severe operating conditions and even during storage [1, 2]. Some positive electrodes may also have a SEI that have a significant contribution such as Ni-rich cathodes [3, 4] and high-voltage $LiCoO_2$ cathodes [5]. This study does not apply to batteries using these cathodes and is focused on batteries with SEI at their anodes.

Tracking the growth of the anode SEI of a LIB over its lifetime would lead to a better follow-up of its state of health, whether it is for scientific studies or for end-users applications. The operating limits of the LIB could be adjusted accordingly as well as its management strategy by its BMS (battery management system). To do this tracking of the SEI growth, advanced characterization methods, non-invasive and suiting a BMS, have to be developed.

The BMS of a battery pack has generally a limited calculation power and basic measuring instruments. It has access to cells voltages, to the battery pack total current and sometimes to some cells surface temperatures. However, BMS sensors accuracy and resolution are often worse than in a laboratory. Also, the major difficulty linked to the SEI-growth tracking is its contribution to a cell voltage is mixed together with the contributions of numerous other phenomena that occur inside an operating battery [6].

Separating the contributions to a battery voltage can be done thanks to an electrical model. To that end, electrochemical models, based on the Newman approach, are interesting because they are based on physical equations. They are made of a set of differential and algebraic equations (DAEs) that brings a good description of electrochemical phenomena at the microscopic scale [7, 8]. The resolution of these coupled DAEs may require a lot of computer-power that would hardly suit a BMS capabilities. Moreover, they contain up to tens of physical parameters that are determined by non-invasive and invasive methods, which can make electrochemical models hard to recalibrate for tracking the SEI-growth in a final-user application.

An equivalent circuit model (ECM) only contains a few parameters that can be determined in a non-invasive way, making them suitable to model commercial batteries with little knowledge of their internal compositions. Besides, they can easily be used with low calculation capabilities like in a BMS. However, the drawback of their simplicity is that the physical phenomena are lumped and are often

*Corresponding author
Email address: nicolas.damay@utc.fr (Nicolas Damay)

mixed together inside "macroscopic" parameters, making their interpretation uncertain.

Nevertheless, many studies have proved that it is possible to find a physical interpretation for ECM parameters. Mauracher *et al.* [9] build a lead-acid battery model with a strong physical background and obtained a good correspondence with experimental data. Von Srbik *et al.* [10], Raël and Hinaje [11] have successfully constructed ECM based on equations that are used classically in electrochemical models.

It is relatively easy to separate the contributions of diffusion phenomena from of other phenomena contributions, because their dynamics is significantly slower [9]. Concerning the contributions of ohmic drops, charge transfers at both electrodes and SEI, they are much harder to separate. More particularly, the charge transfers, associated with the corresponding double layer effects, have dynamics that are very close to the SEI dynamic and they often cannot be distinguished within an impedance spectrum [6]. Illig *at al.* [12] proposed an interesting approach to separate the contributions of several phenomena measured by EIS (electrochemical impedance spectroscopy) thanks to the study of their activation energies (related to their non-linearities regarding temperature), but they could not separate the SEI and charge transfer contributions for the anode.

In this article, we propose a method to separate the contributions of charge transfers and anode SEI that are mixed inside an ECM parameter: the so-called "surface resistance". This method requires EIS and GITT (galvanostatic intermittent titration technique) tests to measure the surface resistance for different temperatures and currents [13, 14]. Then, the non-linearities regarding current and temperature of the charge transfers and SEI contributions are modeled in order to separate them.

The proposed method is applied to a commercial $LiFePO_4$/graphite cell (40 Ah, maximum continuous discharge is 2C), for which the separated contributions of charge transfers and SEI are presented. The non-linearities regarding state of charge (SoC) have been studied in a previous work for this cell [15]. More particularly, we found that its surface resistance does not significantly change with SoC. Consequently, the SoC influence on the proposed method is not studied in this article. The interested reader may refer to the study of Kremer *et al.* [16] which is about SoC-dependency of the charge transfer process, modeled by a SoC-dependency of the exchange current.

In the next section is presented the ECM construction, along with the modeling of the non-linearities regarding current and temperature for the parameter that represents charge transfers and SEI contributions. The experimental determination of this parameter, thanks to EIS and GITT tests, is presented and applied to the studied cell in section 3. In section 4, the separation of the charge transfers and SEI contributions is done for the studied battery and discussed. The eventual use of the proposed non-linearity model with a BMS is also discussed.

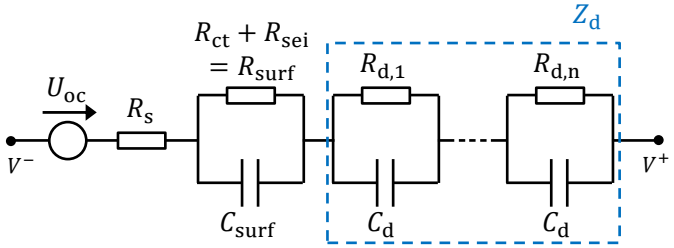

Figure 1: Electrical circuit model used for this study.

2. Battery and surface-resistance non-linearities models

2.1. Electrical circuit model presentation

The ECM used in this study, presented on Figure 1, is composed of several elements that represent the main dynamics and the associated phenomena occurring during a cell operation [17]:

- a voltage source U_{oc} stands for the OCV (open circuit voltage), which is defined as the battery voltage in open circuit and at equilibrium ;
- a resistance R_s represents all the purely resistive contributions (electrolyte, current collectors, contact resistances) ;
- a resistance R_{surf} which is related to the potential drops between the surface of active materials and the electrolyte (mainly due to charge transfers at both electrodes and to the SEI) ;
- a time constant τ_{surf} accounts for the quick dynamic (often inferior to 1 s) associated with charge transfers, double layers and SEI [12, 2]. It is assumed to be a first order dynamic that corresponds to the product $R_{surf} \times C_{surf}$;
- an equivalent diffusion impedance Z_d that reproduces the apparent electrical behavior due to the charges diffusion in the electrolyte and lithium atoms diffusion in the active materials [9, 10, 18].

It has been demonstrated in a previous work that the "slow polarization process" of the studied cell, which is associated with Z_d, behaves like a one-dimensional limited diffusion phenomenon [19]. This corresponds to a Warburg-like behavior that evolves into a purely resistive contribution after a few minutes. Three different diffusion processes can be considered, namely the diffusion of lithium atoms in the active materials of both electrodes [18] and the diffusion of lithium ions in the electrolyte [10, 11]. Nevertheless, grouping them into a single equivalent "limited-diffusion impedance" Z_d gives a satisfactory representation of the studied cell behavior. In the Laplace domain, this leads to a Nernst impedance (Equation (1)) in which Z_d is a function of a "diffusion resistance" R_d and a "diffusion time constant" τ_d [20].

$$Z_d(s) = R_d \,.\, \frac{\tanh(\sqrt{\tau_d.s})}{\sqrt{\tau_d.s}} \tag{1}$$

Equation (1) can be rewritten thanks to Mittag-Leffler theorem to bring Equation (2) [21]. It allows a decomposition of Z_d into an infinite number of RC circuits in series (Figure 1).

$$Z_d(s) = \frac{R_d}{\sqrt{\tau_d.s}} \sum_{p=1}^{\infty} \frac{2\sqrt{\tau_d.s}}{\tau_d.s + (p\pi - \pi/2)^2} \tag{2}$$

This relation can now be rewritten to find the values of the RC circuits parameters : $R_{d,p}$ and $C_{d,p}$ ($\tau_{d,p} = R_{d,p} \times C_{d,p}$).

$$\begin{aligned} Z_d(s) &= \sum_{p=1}^{\infty} \frac{8\,R_d}{4\,\tau_d.s + \pi^2(2p-1)^2} \\ &= \sum_{p=1}^{\infty} \frac{R_{d,p}}{1 + \tau_{d,p}.s} \end{aligned} \tag{3}$$

Which finally yields:

$$\begin{aligned} R_{d,p} &= \frac{8\,R_d}{\pi^2(2p-1)^2} \qquad \tau_{d,p} = \frac{4\,\tau_d}{\pi^2(2p-1)^2} \\ C_{d,p} &= C_d = \frac{\tau_{d,p}}{R_{d,p}} = \frac{\tau_d}{2\,R_d} \end{aligned} \tag{4}$$

Please note that Equation (3) requires an infinite number of RC cells to perfectly match Equation (1). However, because of calculation constraints, the number of RC cells n has to be reduced [21]. The removed RC cells are the ones with a high p value, that is with a short time constant $\tau_{d,p}$ (Equation (4)). Consequently, the precision of the diffusion model is reduced for high frequencies (for very fast current changes), which is acceptable for this study. The number of RC cells n has been set to 10 in this study.

The focus of this study is on the R_{surf} parameter and on the physical information that can be extracted from it, but the determination of the other parameters is important because their contributions are combined together within a battery behavior and all of them have to be considered in order to isolate the one from R_{surf}.

2.2. Modeling the surface resistance R_{surf} non-linearities regarding current

The surface resistance is related to three main contributions, namely the charge transfer processes for both electrodes and the SEI (see section 2.1). The charge transfer processes behaviors are assumed to be indistinguishable from each other. They can be modeled by Equation (5) which is inspired by the Butler-Volmer equation, with I the current flowing through the active materials surfaces (this current is the cell current here), I_0 the exchange current, β the charge-transfer coefficient, V_{ct} the charge transfers overpotential, F the Faraday's constant, R the gas constant and T the absolute temperature [22, 23]. It should be noted that the Butler-Volmer equation is originally defined as the description of a local phenomenon. It is here applied to the whole electrode surface, which implies that the current density and the charge transfers overpotential are assumed to be uniform.

$$I = I_0 \left[\exp\left(\frac{(1-\beta)F}{RT} V_{ct} \right) - \exp\left(\frac{-\beta F}{RT} V_{ct} \right) \right] \tag{5}$$

The contribution of the SEI can be related to the V_{ct} expression with respect to Equation (6) [22]. V_{surf} is thus the potential difference between the solid phase (active materials) and the liquid phase (electrolyte) and R_{sei} is the resistive contribution of the SEI.

$$V_{ct} = V_{surf} - I \times R_{sei} \tag{6}$$

The charge transfer coefficient β is here assumed to be equal to 0.5 [22, 23], leading to a more compact form of Equation (5).

$$I = 2\,I_0 \sinh\left(\frac{F}{2\,RT} \left(V_{surf} - I \times R_{sei} \right) \right) \tag{7}$$

Equation (7) is inverted and divided by the current I to compute the surface resistance R_{surf}, which is the sum of the SEI resistance R_{sei} and an expression corresponding to the charge transfers. For the sake of simplicity, the expression corresponding to charge transfers is called "charge transfers resistance" R_{ct}. The latter is thus non-linear with respect to the current.

$$\begin{aligned} R_{surf}(I) &= \frac{V_{surf}}{I} = R_{sei} + \frac{2\,RT}{F\,I}\, asinh\left(\frac{I}{2\,I_0} \right) \\ R_{surf}(I) &= R_{sei} + R_{ct}(I) \end{aligned} \tag{8}$$

Equation (8) is the foundation of the model proposed in this study. In the next subsections, the temperature dependencies of R_{sei} and R_{ct} are detailed and justified.

2.3. Modeling R_{surf} non-linearities regarding temperature

2.3.1. Presentation of the Arrhenius law

As it is explained in the next subsections, the thermal dependencies within Equation (8) are related to thermally activated processes. Consequently, the Arrhenius law can be used (Equation (9)). k corresponds to a reaction rate at the absolute temperature T (expressed in Kelvin), A is a pre-exponential factor, E_a is the activation energy of the considered reaction (expressed in eV) and k_B is the Boltzmann constant (expressed in eV/K). The universal gas constant R can be used instead of k_B, thus changing the unit of the activation energy E_a.

$$k = A \times e^{-E_a/k_B\,T} \tag{9}$$

Equation (9) has been originally created to describe the temperature dependence of a reaction rate, but it has been found that a lot of thermally activated processes evolves with respect to this formula [12, 24].

2.3.2. Thermal dependency of the charge transfers resistance R_{ct}

The charge transfers resistance depends on the exchange current I_0 (see Equation (8)), which is considered as constant in many works [9, 22, 23]. However, its detailed expression exhibits a dependence to a reaction rate, which is known to evolve with respect to the Arrhenius law (see section 2.3.1) [25]. This was confirmed by measurements made by Takahashi *et al.* [26] on a $LiFePO_4$ electrode. Therefore, I_0 can be replaced by the following expression, with $I_0(25°C)$ the exchange current value at 25 °C and E_{a,I_0} its activation energy. Equation (10) is derived from Equation (9), but it has been normalized so the exponential term equals one at 25 °C.

$$I_0(T) = I_0(25°C) \times \exp\left(\frac{-E_{a,I_0}}{k_B}\left(\frac{1}{T} - \frac{1}{298}\right)\right) \quad (10)$$

2.3.3. Thermal dependency of the SEI resistance R_{sei}

The SEI resistance R_{sei} is also temperature dependent. The diffusivity in a SEI layer depends on temperature in accordance with the Arrhenius law [27], making its conductivity temperature dependent [28, 29]. In this study, the SEI resistance is thus modeled by Equation (11) with $R_{sei}(25°C)$ being the resistance value at 25 °C and $E_{a,sei}$ its activation energy.

$$R_{sei}(T) = R_{sei}(25°C) \times \exp\left(\frac{E_{a,sei}}{k_B}\left(\frac{1}{T} - \frac{1}{298}\right)\right) \quad (11)$$

2.3.4. Complete non-linearities model for R_{surf}

As a result, we propose Equation (12) to model the current and temperature non-linearities of the surface resistance R_{surf}. The latter is considered as the sum of two contributions, namely the SEI resistance R_{sei} and the charge transfers resistance R_{ct}. It uses four parameters: two for the SEI contribution and two for the charge transfers (which are related to the exchange current I_0).

$$R_{surf}(I,T) = R_{sei}(T) + R_{ct}(I,T)$$

$$R_{surf}(I,T) = R_{sei}(25°C) \times \exp\left(\frac{E_{a,sei}}{k_B}\left(\frac{1}{T} - \frac{1}{298}\right)\right) + \frac{2\,R\,T}{F\,I}\,asinh\left(\frac{I}{2\,I_0(25°C)}\exp\left(\frac{E_{a,I_0}}{k_B}\left(\frac{1}{T} - \frac{1}{298}\right)\right)\right) \quad (12)$$

3. Characterization of the surface-resistance non-linearities

3.1. Experimental conditions

A prismatic commercial $LiFePO_4$/graphite cell (40 Ah, maximum 2C for continuous discharge and 1C for continuous charge) was put into a climatic chamber to control its equilibrium temperature. A Bio-Logic system was used for tests (VSP-300), with a 20 A booster for current values of 20 A and below. For higher currents, we used a 100 A booster. The precision of these devices is 0.1% of their full scales. The presented model parameters have been extracted from EIS (Electrochemical Impedance Spectroscopy) and GITT (Galvanostatic Intermittent Titration Technique) tests for different operating conditions.

During an EIS test, a sine wave is applied to the battery and the variation of the voltage is divided by the variation of the current in order to compute the impedance of the battery. This process is repeated for different frequencies in order to get the impedance spectrum of the battery. For this study, EIS tests have been performed at -5 °C, 5 °C, 15 °C, 25 °C and 45 °C, with a C/10 current, at 50% SoC and from 1 kHz to 10 mHz, with 6 frequencies measured per decades.

A GITT test is a repetition of constant-current pulses separated by rest periods (1 h was used or this study). The electrical parameters can be extracted from each pulse, allowing their determination as a function of the SoC. By repeating this process for different currents and temperatures, a characterization of the cell on its whole operating range can be achieved.

GITT tests have been performed at the same temperatures and for the following currents : -100 A (2,5C discharge), -80 A, -60 A, -40 A, -20 A, -10 A, -4 A, -2 A, -1 A, 1 A, 2 A, 4 A, 10 A, 20 A and 40 A (1C charge). They were made between SoC 62,5% and 87,5%, because the OCV curve is flat there, that is on a plateau that allows a better separation of OCV and overvoltage.

It is reminded that the SoC dependency has been already studied for this $LiFePO_4$/graphite cell (40 Ah) and is not considered here [15].

3.2. R_{surf} determination based on EIS for near-zero currents

The Nyquist plots of the obtained impedance spectra are represented on Figure 2a and there is a zoom on the high frequencies values area on Figure 2b.

The sum $R_s + R_{surf}$ is determined in the middle frequencies range (around 1 Hz and 10 HZ), where the arc of a circle returns toward the real axis and the imaginary part of the impedance reaches a local minimal value. There, the real part of the impedance value is considered to be equal to $R_s + R_{surf}$. This process is used for each temperature.

In order to isolate R_{surf} for a given temperature, the R_s parameter value is required. It is assumed to correspond to the minimal real value of the impedance spectrum as represented on Figure 2b [30]. This method has

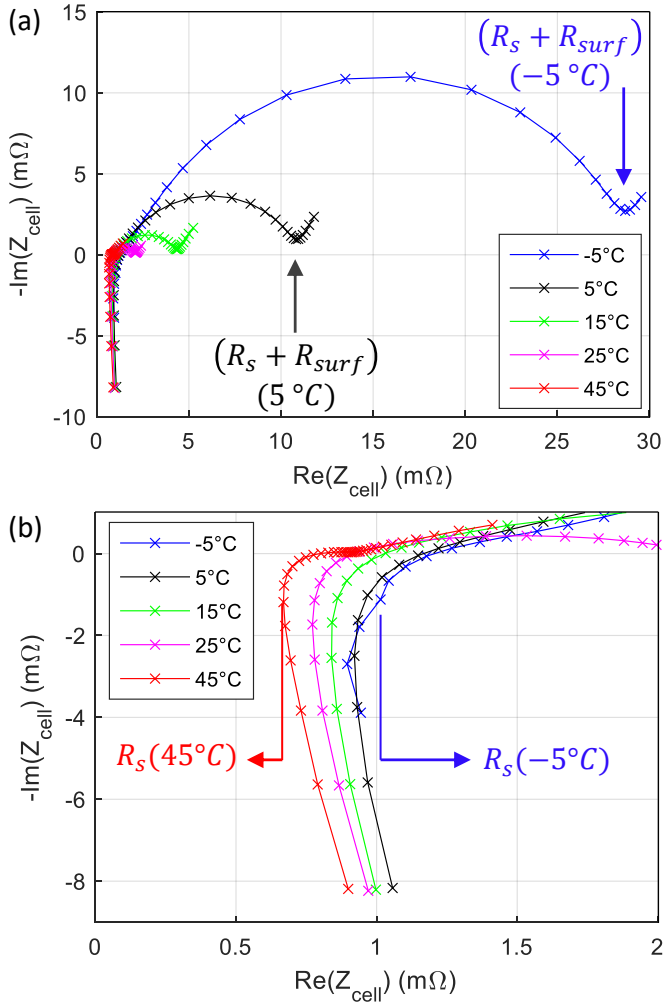

Figure 2: Examples of parameters R_s and R_{surf} extraction from EIS results at different temperatures, from 10 kHz to 10 mHz with 6 points per decade. (a) All impedance spectra and (b) zoom on the high frequencies values area.

been satisfactory for the temperatures between 5 °C and 45 °C. By considering the shapes of the spectra for positive temperatures as references, we chose to consider three EIS values as outliers for the highest frequencies at -5 °C. Consequently, we used the fourth EIS value at -5 °C to determine R_s as represented on Figure 2b.

3.3. R_{surf} determination based on GITT

Extracting R_{surf} from a GITT test requires to separate different contributions to the battery voltage, as stated in the introduction. A typical voltage response of a $LiFePO_4$/graphite cell to a GITT current-pulse has been reproduced on Figure 3 as a function of the time. The OCV and all of the five parameters, including R_{surf} can be extracted from this curve by fitting the ECM of Figure 1 to the voltage response [19].

- U_{oc} is the voltage value before the current pulse, assuming the cell is at equilibrium (measured) ;

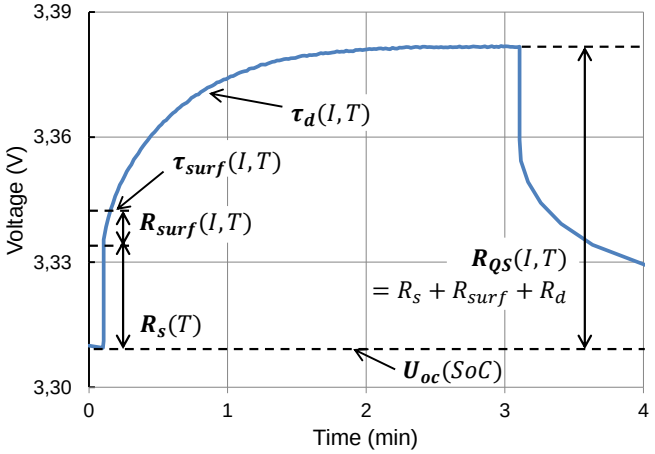

Figure 3: Example of parameters extraction from a GITT result for the studied cell. Their determination is made for several current and temperature values.

- R_s is the instantaneous voltage change at the very beginning of the pulse (this value is extracted from EIS measurements, see section 3.2) ;
- R_{surf} is the overvoltage related to the fast dynamic that occurs during the first tenths of second of the pulse (obtained by fitting);
- τ_{surf} corresponds to the same fast dynamic at the beginning of the pulse (obtained by fitting) ;
- R_d is measured indirectly from the quasi-steady state resistance R_{QS} (Equation (13)), the latter being calculated using the overvoltage value at the end of the pulse (assuming it was long enough for a quasi-steady state to be reached) [19]. This result is used as an initial value for the model fitting.
- τ_d is determined from the voltage response dynamic (obtained by fitting) ;

$$R_{QS}(SoC,T) = R_s(SoC,T) + R_{surf}(SoC,T) + R_d(SoC,T) \quad (13)$$

For this study, the focus is to determine R_{surf} in the most accurate way. It has to be noted that a long GITT pulse voltage-response may not correspond exactly to the diffusion dynamic of the ECM and, thus, that the determination of the diffusion part may be biased. This can lead to a biased determination of R_{surf} and τ_{surf}. To avoid this potential issue, we chose to fit the ECM only on the first 20 seconds of the pulse voltage-response (Figure 4). We used this time frame for the diffusion process to be sufficiently long for it to be fitted easily, but short enough for the voltage response not to be "deformed". Considering that the fit is done only on the first 20 s of the pulse, it is assumed that the cell temperature remains constant and is equal to the climatic chamber temperature.

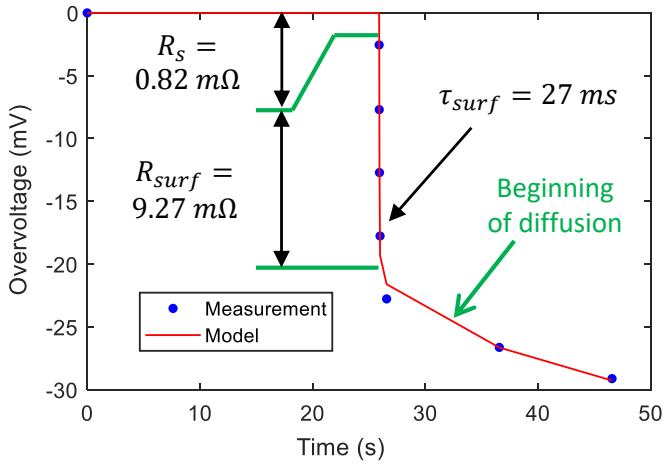

Figure 4: Example of parameters extraction from the beginning of a GITT result for the studied cell (discharging pulse at C/20, 5 °C, between SoC 62.5% and 87.5%).

The example of the Figure 4 represents the surface resistance determination for a discharging pulse at C/20 (2 A), 5°C. The resistance R_s that has been extracted from EIS is reported on the curve, along with the value R_{surf} determined by fitting the ECM to the measurements. Unsurprisingly, the latter is close to the value obtained thanks to EIS, that is 9.65 $m\Omega$. The τ_{surf} value of 27 ms corresponds to a characteristic frequency of 6 Hz that is in accordance with the corresponding frequency range in the EIS data. The fast dynamic of diffusion at the beginning of the pulse is in accordance with theory (see the end of subsection 2.1).

Some operating points of the GITT tests lead to an overvoltage inferior to 10 mV for first few seconds of the pulse and the ECM could not be fitted properly to these measurements. This corresponds to the following operating conditions: 1 A at 5 °C, 2 A and below at 15 °C, 4 A and below at 25 °C, 4 A and below at 45 °C. These points from GITT cannot be used, but this is compensated by the EIS data that provide a good characterization at low current.

4. Separating charge transfers an SEI contributions of a $LiFePO_4$/graphite cell

4.1. Fitting the proposed non-linearities model to the experimental data

The results of the R_{surf} determination (by EIS and GITT) are presented on Figure 5 for different temperatures and as functions of the current (positive current values are for charging conditions). The experimental values extracted from GITT are represented by circles and the ones from EIS are represented by triangles. There is a good correspondence between EIS and GITT results for near-zero currents. These data have been fitted to the model proposed in this study (Equation (12)) and the optimized model predictions have been represented as solid lines on Figure 5.

There is a good agreement between the data and the proposed model (root mean squared error is 0.33 $m\Omega$). The fitting parameters have been reported in Table 1. The values of the parameters at 25 °C are 0.47 $m\Omega$ for R_{sei} and 32.5 A for the exchange current I_0. The corresponding "charge transfers resistance" $R_{ct,0}$ at 25 °C, as it is defined for EIS analysis for a near-zero currents (see Equation (14)), is 0.79 $m\Omega$ [29]. Considering that the studied battery is already several years old, it is not surprising to find a SEI resistance that is significant compared to the charge transfers resistance. Finally, the sum of R_{sei} and $R_{ct,0}$ is 1.26 $m\Omega$, which is close to the measured value by EIS (5% lower than 1.33 $m\Omega$).

	Value at 25 °C	Activation energy
R_{sei}	0.47 $m\Omega$	0.59 eV
I_0 ($R_{ct,0}$)	32.5 A (0.79 $m\Omega$)	0.81 eV

Table 1: Fit parameters for the surface resistance R_{surf} model of the Figure 5a, corresponding to Equation (12). The calculus of $R_{ct,0}$, corresponding to Equation 14, is included.

$$R_{ct,0}(T) = \frac{RT}{FI_0(T)} \tag{14}$$

The activation energy $E_{a,sei}$ related to R_{sei} is 0.59 eV, which is close to the value found in literature (0.52 eV according to Pinson *et al.* [27]). The activation energy E_{a,I_0} related to I_0 is 0.81 eV, which is higher than the values reported in the literature (between 0.52 to 0.73 eV [29, 31, 32, 33]). This could be explained by the way the values found in the literature have been measured and we discuss this in the section 4.2. Based on the results, we consider that the model proposed in this study is experimentally validated.

The contributions of the charge transfers and the SEI to the battery voltage have been represented on Figure 6 by the corresponding non-linear resistances, respectively R_{ct} and R_{sei} (see Equation (12)). According to the proposed model, the charge transfers contribution R_{ct} is the largest for near-zero currents. For the studied battery, R_{ct} does not significantly depends on current at 25 °C and 45 °C. However, at 15 °C and for lower temperatures, it decreases quickly when the current increases. Consequently, the SEI contribution R_{sei} becomes the largest at low temperatures (5 °C and below) and high currents (1C and above). These operating points are thus interesting for the SEI growth tracking.

4.2. Discussions

The authors would like to emphasize that the activation energies that are measured for the graphite-anode charge-transfer (same as E_{a,I_0} in this study) in the cited

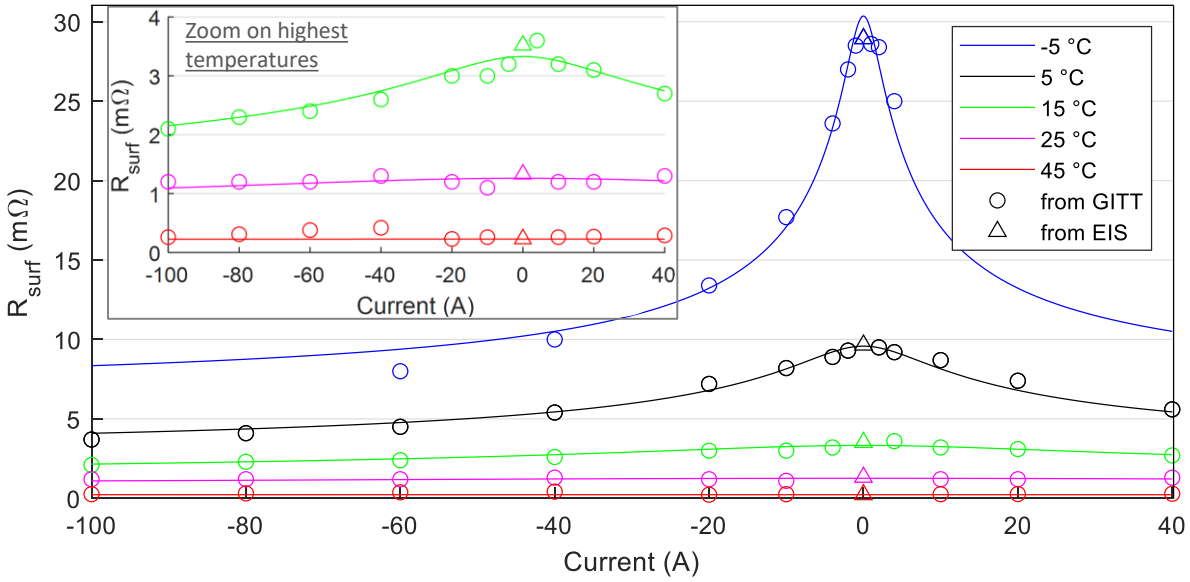

Figure 5: Fitting the experimental surface-resistance values to Equation (12). Solid lines correspond to the model values.

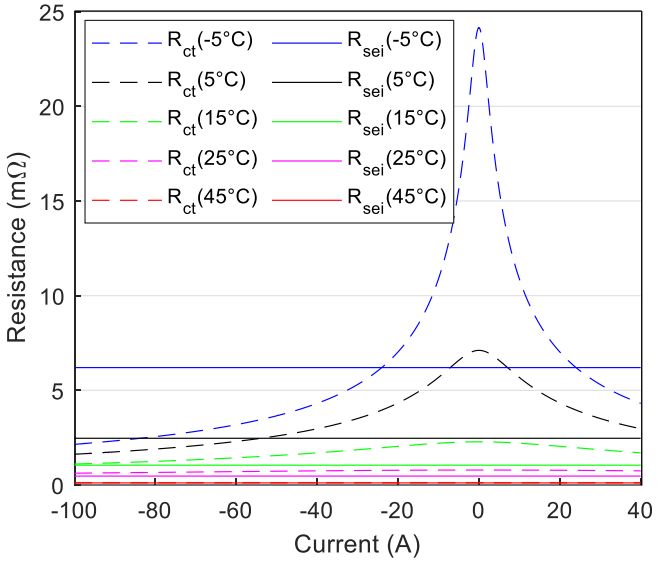

Figure 6: Separated contributions of the charge transfers and the SEI to the battery voltage, represented by the corresponding non-linear resistances R_{ct} and R_{sei}, as functions of the current and for different temperatures.

references embed both charge transfer and SEI contributions to the anode impedance. In order to truly compare our results with the literature, we determined the activation energy related to the R_{surf} values determined by EIS from -5 °C to 45 °C. By fitting these values to an Arrhenius law, we found a so-called surface-resistance activation-energy of 0.71 eV. This value lies in between E_{a,I_0} (0.81 eV) and $E_{a,sei}$ (0.59 eV) and is more in accordance with the literature data (between 0.52 to 0.73 eV [29, 31, 32, 33]). A proper separation of charge transfer and SEI activation energies might lead to higher values for the charge transfer of graphite anodes, like in this study. As the balance between charge transfers and SEI contributions is likely to change during this battery lifetime because of SEI growth, an evolution of the "surface-resistance activation-energy" may occur.

It is noteworthy that the bell-shape of the surface resistance is narrower for lower temperature (Figure 5). At -5 °C, it is so narrow that even values at C/10 (4 A) are significantly smaller than the near-zero currents value of R_{surf}. This makes the EIS measurements questionable, because it has been made with a current amplitude of C/10. Hence, the "small perturbation" hypothesis that is required for EIS measurements could be affected. This could be solved with an EIS test using a sufficiently reduced current for the lowest temperatures. Unfortunately, this could not have been done with the studied cell because his SEI resistance value had already significantly increased by the time we realized this issue. We consider that the possible underestimation of the EIS value at -5°C does not challenge this study conclusions.

From the results of Figures 5 and 6, we can infer that GITT measurements are sufficient to fit the proposed non-linearities model and, thus, to separate charge transfers and SEI. Assuming that an initial calibration of the model is done for a pristine cell and that it is embedded into a BMS, it seems achievable to do an online recalibration of the model parameters based on current pulses at different temperatures during operation (the lowest temperatures being the best). Nevertheless, several factors may impact the extraction quality of R_{surf} from the BMS measurements and would have to be carefully studied, namely: potentially low sampling frequency, sensors accuracy, measurement noise, inaccurate separation of R_{surf} and the diffusion part (see Figure 4).

5. Conclusion

The contributions of both electrodes charge transfers and of the anode SEI have been associated with one of the parameters of a simple equivalent circuit model (ECM), the so-called surface resistance R_{surf}. The experimental determination of this parameter has been presented. It is based on GITT tests made from C/40 to 2.5C) and on EIS tests for near-zero currents. This experimental characterization has been carried out on a commercial $LiFePO_4$/graphite prismatic cell. The determination of its surface resistance has been done over most of its operating range, from -5 °C to 45 °C and from 2.5C in discharge to 1C in charge.

A method has been proposed to separate the contributions of charge transfers and SEI that are mixed inside the surface resistance parameter. This method is based on an analytical model of the surface-resistance non-linearities regarding current and temperature. It is inspired by the Butler-Volmer relation in which the SEI contribution has been included in accordance with the literature. The thermal dependencies of the current exchange and the SEI equivalent resistance, using the Arrhenius law, have been justified and included into the non-linearities model.

Using the proposed model, the charge transfers and SEI contributions to the studied cell voltage have been separated with a satisfactory accuracy. They are characterized by their respective values at 25 °C and activation energies, that is four parameters. The activation energies of the SEI and charge transfers resistances are respectively 0.59 eV and 0.81 eV, which is in accordance with literature data. We showed that the contribution of the charge transfers to the surface resistance is major for low currents and low temperatures. Concerning the SEI contribution to the surface resistance, we demonstrated that it is dominant at high current and low temperature for the studied cell.

By construction, the proposed method is not specific to $LiFePO_4$/graphite batteries and should be applicable to other battery electrodes inside of which the same electrochemical phenomena occur. In particular, the proposed approach is based on the assumptions of a negligible cathode-SEI contribution and of charge transfers that do not depend on SoC. By allowing the separation of charge transfers and anode SEI contributions, it allows to track the SEI growth of a battery during its lifetime in a non-invasive way. It would be expected for the activation energies to remain the same but for the SEI resistance, at least, to increase when battery is aging. This article approach may thus be interesting for a finer analysis of a battery state of health during aging studies.

After an initial calibration, the proposed model could be embedded in a BMS and, based on high current pulses at low temperature during the normal operation of a battery, it may be possible to recalibrate the model and thus estimate the SEI or charge transfer resistance evolution.

Acknowledgment

The authors would like to thank Dr. Charles Delacourt for the fruitful discussions about the physical interpretation of ECM.

References

[1] J. Vetter, P. Novák, M. Wagner, C. Veit, K.-C. Möller, J. Besenhard, M. Winter, M. Wohlfahrt-Mehrens, C. Vogler, A. Hammouche, Ageing mechanisms in lithium-ion batteries, Journal of Power Sources 147 (1-2) (2005) 269–281.

[2] M. T. Lawder, P. W. C. Northrop, V. R. Subramanian, Model-Based SEI Layer Growth and Capacity Fade Analysis for EV and PHEV Batteries and Drive Cycles, Journal of the Electrochemical Society 161 (14) (2014) A2099–A2108.

[3] F. Schipper, E. M. Erickson, C. Erk, J.-Y. Shin, F. F. Chesneau, D. Aurbach, Review—Recent Advances and Remaining Challenges for Lithium Ion Battery Cathodes, Journal of The Electrochemical Society 164 (1) (2017) A6220–A6228.

[4] D. Pritzl, A. E. Bumberger, M. Wetjen, J. Landesfeind, S. Solchenbach, H. A. Gasteiger, Identifying Contact Resistances in High-Voltage Cathodes by Impedance Spectroscopy, Journal of The Electrochemical Society 166 (4) (2019) A582–A590.

[5] Dynamic evolution of cathode electrolyte interphase (CEI) on high voltage LiCoO2 cathode and its interaction with Li anode, Energy Storage Materials 14 (February) (2018) 1–7.

[6] J. Illig, J. P. Schmidt, M. Weiss, A. Weber, E. Ivers-Tiffée, Understanding the impedance spectrum of 18650 $LiFePO_4$-cells, Journal of Power Sources 239 (2013) 670–679.

[7] R. Malik, A. Abdellahi, G. Ceder, A Critical Review of the Li Insertion Mechanisms in $LiFePO_4$ Electrodes, Journal of the Electrochemical Society 160 (5) (2013) A3179–A3197.

[8] M. Farkhondeh, M. Pritzker, M. Fowler, C. Delacourt, Mesoscopic Modeling of a $LiFePO_4$ Electrode: Experimental Validation under Continuous and Intermittent Operating Conditions, Journal of The Electrochemical Society 164 (11) (2017) E3040–E3053.

[9] P. Mauracher, E. Karden, Dynamic modelling of lead/acid batteries using impedance spectroscopy for parameter identification, Journal of Power Sources 67 (1-2) (1997) 69–84.

[10] M.-T. Von Srbik, M. Marinescu, R. F. Martinez-botas, G. J. Offer, A physically meaningful equivalent circuit network model of a lithium-ion battery accounting for local electrochemical and thermal behaviour , variable double layer capacitance and degradation, Journal of Power Sources 325 (2016) 171–184.

[11] S. Raël, M. Hinaje, Using electrical analogy to describe mass and charge transport in lithium-ion batteries, Journal of Power Sources 222 (2013) 112–122.

[12] J. Illig, M. Ender, T. Chrobak, J. P. Schmidt, D. Klotz, E. Ivers-Tiffee, Separation of Charge Transfer and Contact Resistance in $LiFePO_4$-Cathodes by Impedance Modeling, Journal of the Electrochemical Society 159 (7) (2012) A952–A960.

[13] K. Onda, T. Ohshima, M. Nakayama, K. Fukuda, T. Araki, Thermal behavior of small lithium-ion battery during rapid charge and discharge cycles, Journal of Power Sources 158 (1) (2006) 535–542.

[14] M. Gholizadeh, F. R. Salmasi, Estimation of State of Charge, Unknown Nonlinearities, and State of Health of a Lithium-Ion Battery Based on a Comprehensive Unobservable Model, IEEE Transactions on Industrial Electronics 61 (3) (2014) 1335–1344.

[15] N. Damay, C. Forgez, G. Friedrich, M.-P. Bichat, Heterogeneous behavior modeling of a $LiFePO_4$-graphite cell using an equivalent electrical circuit, Journal of Energy Storage 12 (2017) 167–177.

[16] F. Kremer, S. Rael, M. Urbain, 1D electrochemical model of lithium-ion battery for a sizing methodology of thermal power plant integrated storage system, AIMS Energy 8 (5) (2020) 721–748.

[17] E. Kuhn, C. Forgez, G. Friedrich, Modeling diffusive phenomena using non integer derivatives, The European Physical Journal Applied Physics 25 (3) (2004) 183–190.
[18] J. Huang, Z. Li, J. Zhang, S. Song, Z. Lou, N. Wu, An Analytical Three-Scale Impedance Model for Porous Electrode with Agglomerates in Lithium-Ion Batteries, Journal of The Electrochemical Society 162 (4) (2015) A585–A595.
[19] N. Damay, C. Forgez, M.-P. Bichat, G. Friedrich, Thermal modeling of large prismatic $LiFePO_4$/graphite battery . Coupled thermal and heat generation models for characterization and simulation, Journal of Power Sources 283 (2015) 37–45.
[20] N. Devillers, Caractérisation et modélisation de composants de stockage électrochimique et électrostatique, Ph.D. thesis (2013).
[21] E. Kuhn, C. Forgez, P. Lagonotte, G. Friedrich, Modelling Ni-MH battery using Cauer and Foster structures, Journal of Power Sources 158 (2) (2006) 1490–1497.
[22] M. Farkhondeh, C. Delacourt, Mathematical Modeling of Commercial $LiFePO_4$ Electrodes Based on Variable Solid-State Diffusivity, Journal of The Electrochemical Society 159 (2) (2012) A177.
[23] K. S. Hariharan, V. S. Kumar, A coupled nonlinear equivalent circuit – Thermal model for lithium ion cells, Journal of Power Sources 227 (2013) 171–176.
[24] S.-Y. Chung, J. T. Bloking, Y.-M. Chiang, Electronically conductive phospho-olivines as lithium storage electrodes., Nature materials 1 (2) (2002) 123–8.
[25] M. Mastali, M. Farkhondeh, S. Farhad, R. A. Fraser, M. Fowler, Electrochemical Modeling of Commercial $LiFePO_4$ and Graphite Electrodes: Kinetic and Transport Properties and Their Temperature Dependence, Journal of The Electrochemical Society 163 (13) (2016) A2803–A2816.
[26] M. Takahashi, S.-i. Tobishima, K. Takei, Y. Sakurai, Reaction behavior of $LiFePO_4$ as a cathode material for rechargeable lithium batteries, Solid State Ionics 148 (2002) 283–289.
[27] M. B. Pinson, M. Z. Bazant, Theory of SEI Formation in Rechargeable Batteries: Capacity Fade, Accelerated Aging and Lifetime Prediction, Journal of the Electrochemical Society 160 (2) (2012) A243–A250.
[28] M. Park, X. Zhang, M. Chung, G. B. Less, A. M. Sastry, A review of conduction phenomena in Li-ion batteries, Journal of Power Sources 195 (24) (2010) 7904–7929.
[29] M. Ecker, S. Kabitz, I. Laresgoiti, D. U. Sauer, Parameterization of a Physico-Chemical Model of a Lithium-Ion Battery: I. Determination of Parameters, Journal of the Electrochemical Society 162 (9) (2015) A1849–A1857.
[30] S. Skoog, S. David, Parameterization of linear equivalent circuit models over wide temperature and SOC spans for automotive lithium-ion cells using electrochemical impedance spectroscopy, Journal of Energy Storage 14 (2017) 39–48.
[31] K. Xu, "Charge-Transfer" Process at Graphite/Electrolyte Interface and the Solvation Sheath Structure of Li^+ in Nonaqueous Electrolytes, Journal of The Electrochemical Society 154 (4) (2007) S9.
[32] T. R. Jow, M. B. Marx, J. L. Allen, Distinguishing Li^+ Charge Transfer Kinetics at NCA/Electrolyte and Graphite/Electrolyte Interfaces, and NCA/Electrolyte and LFP/Electrolyte Interfaces in Li-Ion Cells , Journal of The Electrochemical Society 159 (5) (2012) A604–A612.
[33] H.-j. Liu, Q. Xu, C.-w. Yan, Y.-z. Cao, Y.-l. Qiao, The Effect of Temperature on the Electrochemical Behavior of the V(IV)/V(V) Couple on a Graphite Electrode, International Journal of Electrochemical Science 6 (2011) 3483–3496.